The 8th European Congress on Computational Methods in Applied Sciences and Engineering
ECCOMAS Congress 2022
5-–9 June 2022, Oslo, Norway

# UNCERTAINTIES OF PARAMETERS QUANTIFICATION IN SHM

**Mohammad S. Miah[1,*], and Werner Lienhart[1]**

[1] Institute of Engineering Geodesy and Measurement Systems, Graz University of Technology, 8010 Graz, Austria
*Correspondence to: miah@tugraz.at

**Key words:** Uncertainties, Structural Health Monitoring, Parameters, Sensors Fusion

**Abstract.** The uncertainties of parameters quantification due to various known and unknown conditions are crucial to understand structural health monitoring (SHM) systems. For instance, the amplitudes and the variation of loading conditions play a vital rule how the structural parameters are going to be changed. Hence, the aforementioned issue leads to an additional challenge in the area of SHM that requires attention. This study observed the behaviour of a steel bridge experimentally by employing multi-sensors scenarios e.g. accelerometers and laser triangulation sensor. The dynamical properties such as the peak (e.g. maximum-minimum) accelerations and displacements are evaluated. Additionally, the frequencies and damping ratio from the measured data of the tested bridge has been estimated by utilizing the fast Fourier transform (FFT) estimation. The outcome shows that the variation of input excitations (i.e., random, free-decay, extra-loading) effects the investigated properties as well as on their magnitudes considerably. Therefore, the findings suggest that before making a final judgement based on the identified/estimated properties from measured data, the underlying uncertainties need to be considered to avoid sub-optimal assessment strategy.

## 1 INTRODUCTION

The advancement of modern structural systems and development as well as their fusion with state-of-the-art technologies are noticeable. As a result, designers need to take extra caution to keep those structures safe by employing various monitoring strategies. The monitoring scheme assist to keep a track on the overall structural health condition. And based on the current obtained information of the structures via sensors, decisions can be made or an alarm can be provided to the community. Nevertheless, the inherent uncertainties associated with the structures and technologies e.g. sensors are making the structural health monitoring (SHM) task intricated.

The uncertainties can be induced into the structural response from various sources and in different forms. For instance, the magnitude variation of the input excitation can lead to a devastating situation of the structures as they will lead to significant changes into the amplitudes of the response e.g. displacement, as a result, partial or even full-collapse can occur. In this context, typically, the dynamical systems are treated as linear time-invariant (LTI) systems where the Fourier base transformation works effectively while it may not be suitable for the linear time-variant (LTV) systems [1]. A comparative study by employing various input excitations

have been conducted in [1] and reported that due to the complex natures and variation of the input excitations (e.g. impact, chirp), it is not possible to identify the desired properties of time-variant systems. The unpredictability effect of different input excitations to dynamical systems have been investigated in [2] and their significance was reported. The inherent uncertainties in SHM has been studied by considering cultural heritage buildings under ambient type vibration and also reported that the aforementioned vibration is not suitable to excite effectively in the desired frequency range [3]. Uncertainties can be induced in numerous way into a dynamical system, especially, when the framework deals with identifying, modelling and updating properties of the systems [4, 5].

In literature, many methods can be found which have been implemented and adopted to quantify and estimate uncertainties in SHM. Among many existing approaches to deal with uncertainties, as for example: Gaussian based approach [6], deep-vision [7], Bayesian statistics [8], Bayesian inference [9], limited sensors or information approach [5, 10, 11, 12], state-space autoregressive models [13], Bayesian deep-learning [14], probabilistic approach [15], model-based occupant localization [16], switching state-space autoregressive models [17].

In this context, over the last few decades, researchers are adopting the system identification approach to have robust and smart monitoring of civil structures and infrastructures. The aforementioned strategy leads to on even more complicated situation in terms of uncertainties. This issue has been taking serious attention in the area of SHM and many works have already been adopted and investigate the efficacy of the discussed approach. Among many, a framework was proposed considering the temperature compensation for civil infrastructural applications [18]. An overview with numerical examples to deal with uncertainties in prognosis and SHM are presented in [19]. Furthermore, the system identification was integrated for SHM considering uncertainties [20]. The uncertainties can have various form, for instance, data related unpredictability in SHM was investigated [21].

Herein, this study has focused into the uncertainties based on the measured data. More specifically, typically, structural vibration changes it magnitudes and frequencies depending on the type of input excitation. The aforementioned issue has been the main focuses of this research work. The rest of the paper is organized as: the framework is presented in the immediate next section, afterward, the results are discussed, and the final section contains the summary of the study.

## 2 THE FRAMEWORK

This study investigates the uncertainties of the structural parameters from the measured data under various input excitations. In order to measure the data of two type of sensors are employed and they are (a) accelerometers, and (b) triangulation laser sensor. In brief, the accelerometers are manufactured by PCB and have a resolution of $750\mu$g. While the laser triangulation sensors are manufactured by Micro-Epsilon and have a resolution of $(10^{-4})$ mm. The acceleration data was recorded at a sampling frequency of 4800Hz whereas the displacement data was recorded with a sampling rate of 312.50Hz. Among the key investigation criteria: (i) the absolute maximum peaks of acceleration data, (ii) the absolute maximum peaks of displacements data, (iii) estimating frequencies, and (v) determining damping ratios are considered.

The overall framework consist of (i) data measuring and sorting, (ii) data post-processing

and cleaning, (iii) comparison between raw data and cleaned data, (iv) absolute peaks selection for both acceleration and displacements data, (v) estimation and comparison of frequency spectrum via fast Fourier transformation (FFT), (vi) calculating damping ratio via the half-power bandwidth method.

### 2.1 The half-power bandwidth method

There are many ways to estimate the damping and damping ratio of any dynamical system. Among them the half-power bandwidth method (HPBM) is a quite well-known tool to estimate damping ratio in particular output-only cases (when the input excitation is missing). However, in order to employ the HPBM the frequency spectrum is essential. Herein the frequency spectrum is estimated via the use of fast Fourier transformation. Typically, the FFT is performed in a discrete manner known as the DFT and that is given by,

$$X_k = \sum_{n=0}^{N-1} x_n e^{(-2i\pi kn/N)} \tag{1}$$

where $x_n$ is a complex number, $k$ is a integer number, $N$ sample length, $i$ represents the imaginary variable.

The damping ratio can be estimated via the expression given below by using the half-power bandwidth method.

$$\begin{aligned} Q &= \frac{1}{2\zeta} \\ \zeta &= \frac{f_{max} - f_{min}}{2f_n} \end{aligned} \tag{2}$$

where $Q$ represents the quality factor, $\zeta$ is the damping ratio, $f_{max}$ and $f_{min}$ are the maximum and minimum frequencies of the bandwidth, $f_n$ is the natural frequency.

For better understanding, a graphical representation of the half-power bandwidth method is depicted in Figure 2.1. The following article [22] can be recommended for further detailed information regarding the half-power bandwidth method.

## 3 RESULTS AND DISCUSSION

The goal of this study has been achieved by evaluating measured acceleration and displacement data. Both the acceleration and displacements results are discussed in this section. The data was recorded under various loading conditions such as applying random impulse type vibration via figure tips. In addition to random impulse, extra weights are placed on the bridge to create an extreme scenario. And data have measured considering two different support conditions: (i) hinge-roller, and (ii) roller-fixed. Due to the space limitation, only important results of acceleration data are presented for both support conditions (hinge-roller and hinge-fixed). Meanwhile, in case of displacements, the results are discussed only for the roller-fixed type support condition.

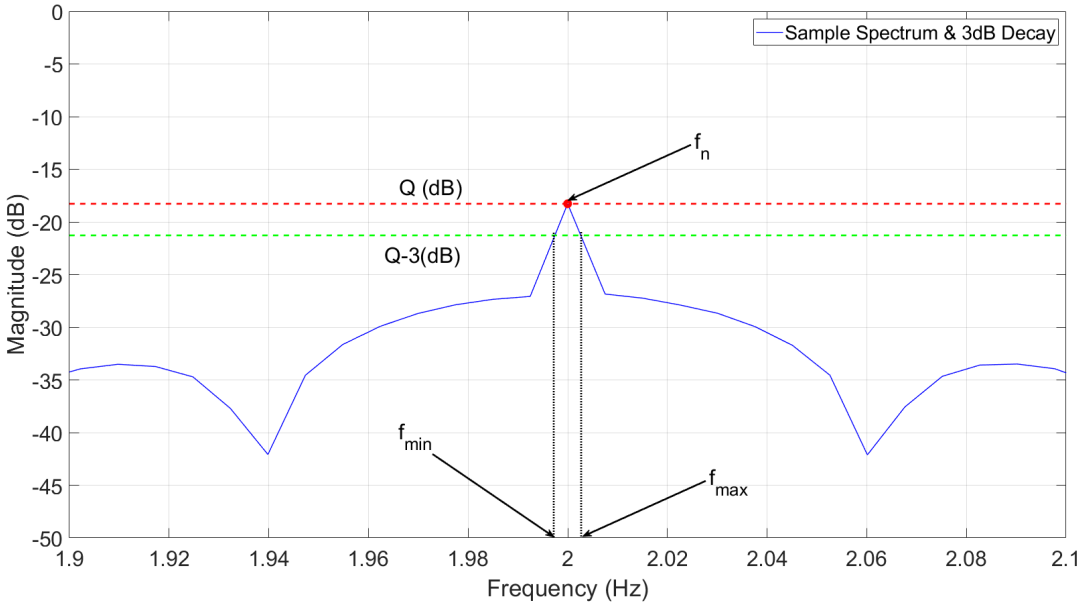


**Figure 1**: Sample spectrum to illustrate 3dB decay for the half-power bandwidth method

### 3.1 Evaluation of the Acceleration Data

It is mentioned earlier that the acceleration data has been recorded by employing PCB uni-axial type accelerometers. And the data has been measured with a sampling frequency of 4800Hz. Initially, the results are evaluated for the support condition of hinge-roller and presented in Figures 2 - 4. While in the later part of this section has covered the results of the roller-fixed support condition and depicted in Figures 5 - 6.

A sample set of measured time history of acceleration data is shown in Figure 2. One may notice that the top sub-figure shows the full-series, whereas, the rest of the sub-figures (e.g. Peak 1, Peak 2, etc.) show a specific selected time-window data (see the x-axis of the sub-figures). The aforementioned figures show the overall variation of the maximum and minimum peak values under different loading conditions for hinge-roller support. Further, the maximum and minimum values of all peaks have been evaluated and presented in Figure 2. Figure 2 shows the changes of the magnitude of the accelerations for different loading conditions. In other words, it can be said that the applied loads can change the maximum and minimum values significantly. Additionally, for more clear understanding a summary of maximum and minimum acceleration values have been provided in Table 1 for both support conditions.

Further, in a first step, the comparison of the time and frequency domain results have been presented in Figure 3. This figure provides the fundamental/resonant frequency information of the bride. In the next step, all the selected time-window data has been evaluated and depicted in Figure 4. Interestingly, it can be easily seen that the natural frequency has been shifted significantly due to the variation of the input excitations.

Similarly, the measured accelerations data are evaluated for the fixed-roller support condition

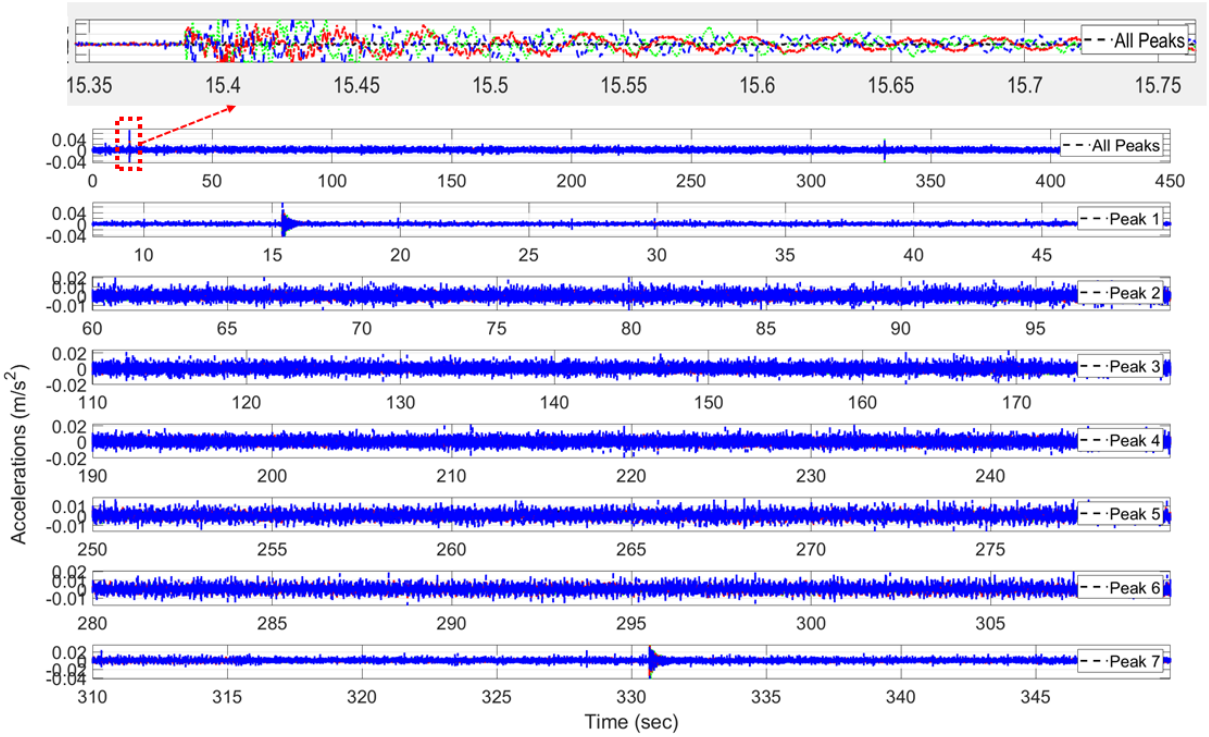


**Figure 2**: Time series data of acceleration showing all peaks and selected time-windows under hinge-roller support condition

subjected to different input excitations as before. Firstly, a sample set of acceleration time-series data has been depicted in Figure 5. In the early mentioned figure (e.g. Figure 5), the top sub-figure shows the entire measured data-series, and the rest of the sub-figures (e.g. Peak 1, Peak 2, etc.) show the selected time-window data only. For better understanding, see the x-axis of the sub-figures of Figure 5. And ones may easily notice that the maximum and minimum peak values have changed significantly due to variation of the input loads also for support conditions.

To interpret more clearly, the maximum and minimum values of all peaks (e.g. Peak 1, Peak 2, so on) are summarized in Table 1. It can be easily found in the early mentioned figure that the difference in the magnitude of the maximum and minimum peak values of accelerations. Similar to the early discussed case (e.g. hinge-roller), it can be summarized that the variation of input excitations may lead to significant changes on the overall dynamics as well as on the magnitudes.

Later, the frequency spectrums for all the selected time-window data have been derived in Figure 6 and the it can be seen that the resonant frequency has been shifted substantially with the changes of the input loads.

### 3.2 Evaluation of the Displacement Data

The results obtained from displacements data are discussed in this section. The data has been recorded via the use of a laser triangulation sensor (LTS) that has a resolution of $1e^{-}5$

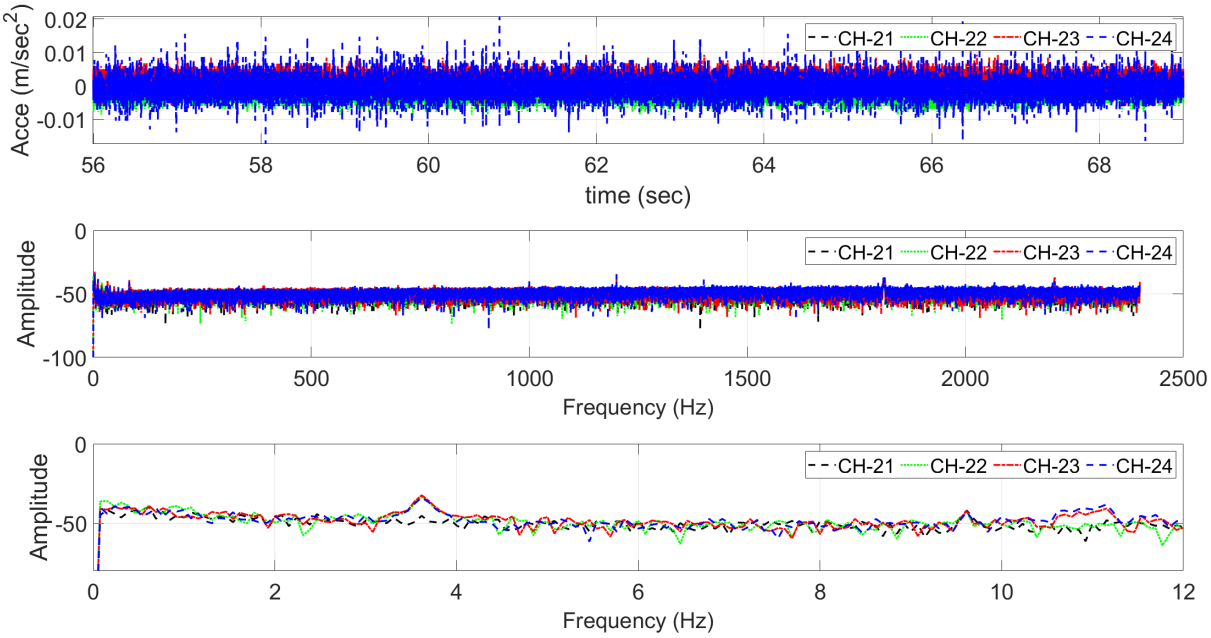


**Figure 3**: A sample set of results of reference (no extra weight on the bridge) case under hinge-roller support condition

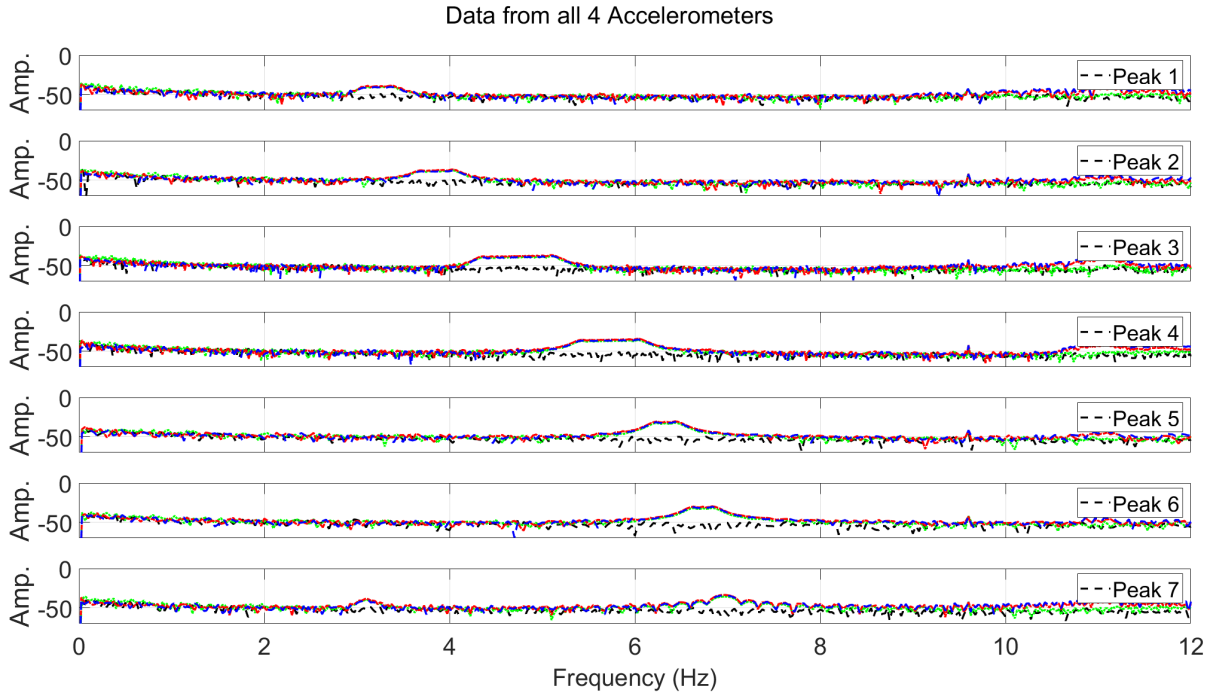


**Figure 4**: Comparison of spectrums of all considered time-windows under hinge-roller support condition

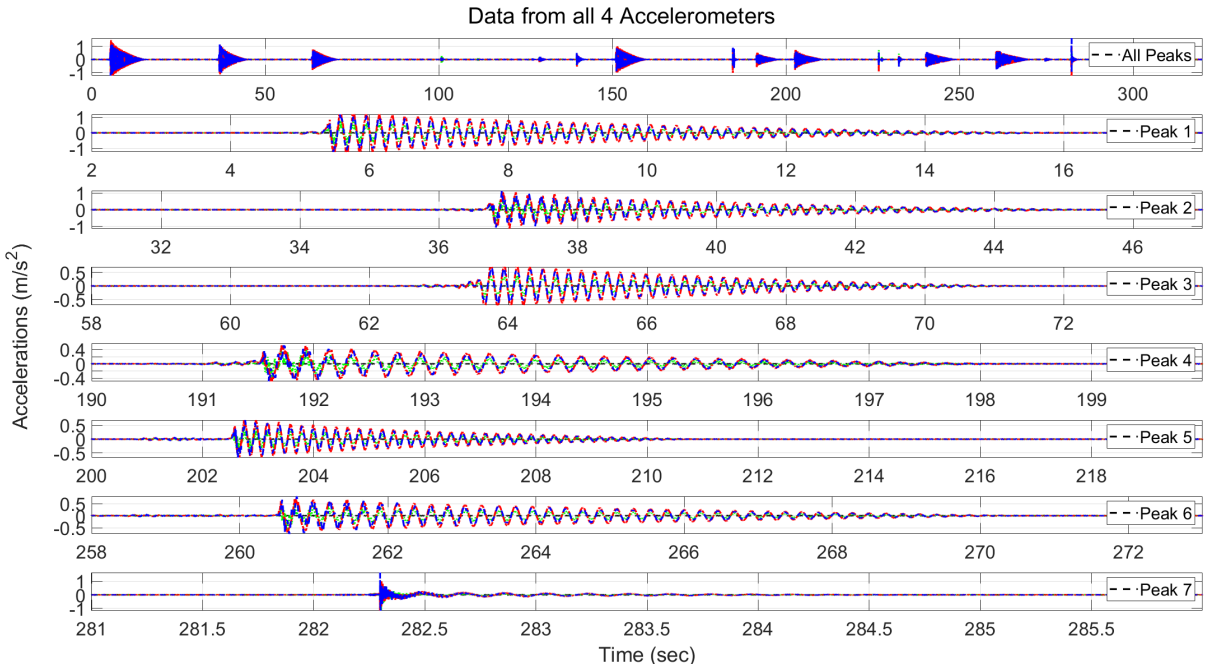


**Figure 5**: Time series data of acceleration showing all peaks and selected time-windows under fixed-roller support condition

**Table 1**: Maximum and minimum peak accelerations under hinge-roller and fixed-roller support cases

| Peaks | Hinge-roller support cases | Fixed-roller support case |
|---|---|---|
| Acceleration | Maximum-Minimum $(m/s^2)$ | Maximum-Minimum $(m/s^2)$ |
| Peak 1 | 0.077 - 0.047 | 1.193 - 1.233 |
| Peak 2 | 0.021 - 0.016 | 1.148 - 1.147 |
| Peak 3 | 0.024 - 0.020 | 0.695 - 0.696 |
| Peak 4 | 0.022 - 0.020 | 0.578 - 0.491 |
| Peak 5 | 0.019 - 0.016 | 0.693 - 0.668 |
| Peak 6 | 0.021 - 0.018 | 0.802 - 0.752 |
| Peak 7 | 0.036 - 0.043 | 1.632 - 1.168 |

mm and the sampling frequency of the LTS was 312.50 Hz. It is mentioned earlier that for the LTS sensor data only fixed-roller case is presented herein. To be consistent, the results are presented in a similar manner as acceleration data. The measured time-series data is presented in Figure 7, where a sample full-series (see top sub-figure) along with selected time-windows in sub-figures can be observed. Most importantly, the difference in the magnitudes of different time-windows can be noticed and Figure 8 may provide further detail in this matter.

Before jump into the final spectrum comparison, a sample spectrum has been estimated to evaluate the resonant frequency from LTS data shown in Figure 9. Afterward, the frequency

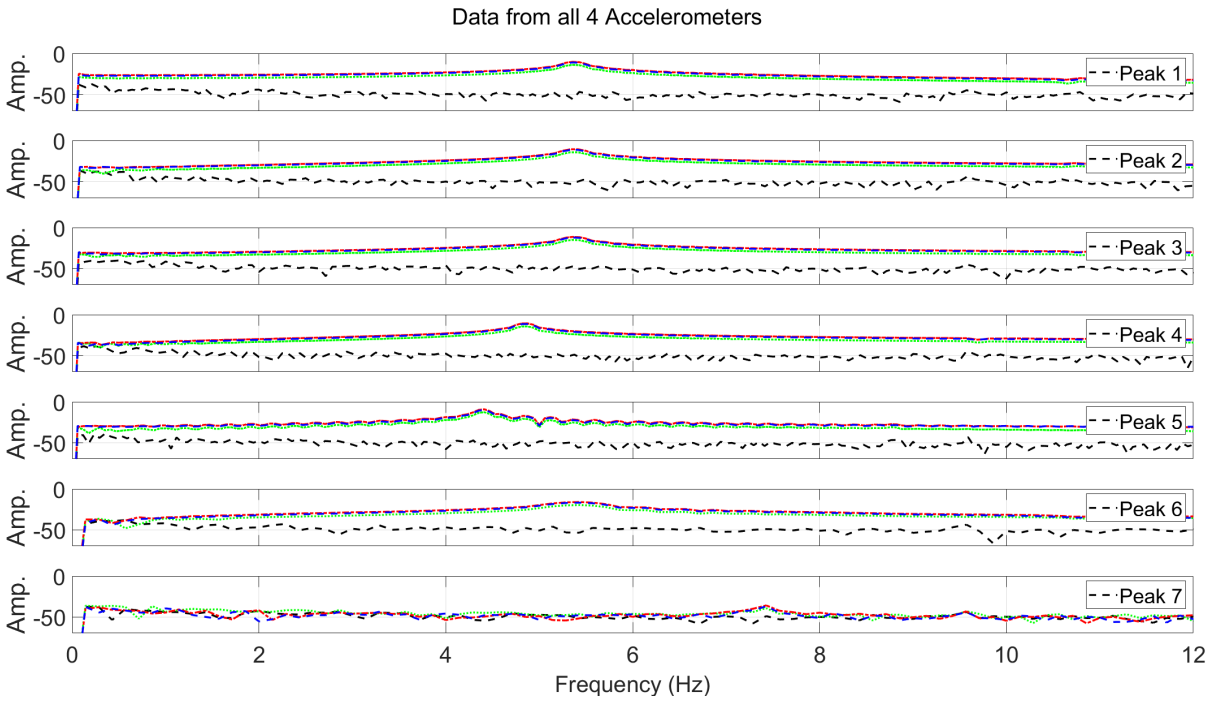


**Figure 6**: The comparison of spectrums of all considered time-windows under fixed-roller support condition

spectrums for all considered time-windows have been prepared and presented in Figure 10. From the aforementioned figure, the shift of the natural frequency is clearly visible. In a nutshell, this can be summarized from all the results presented in this study is that the magnitudes and the important dynamic properties e.g. natural frequency may change significantly due to the variation of the supports and input excitations.

Last but not least, the damping ratio for all those selected time-windows of acceleration and displacement data are estimated and presented in Table 2. Where, also similar results have been found that the damping ratio may also change due to the changes of supports and input excitations. Interestingly, the estimated damping ratios from different signals (acceleration and displacements) agreed quite well, especially, when bridge is subjected to vibration only (without extra weight on it).

## 4 CONCLUSIONS

This study investigates the deviation of the dynamical properties of a steel bridge via the use of measured acceleration and displacement data. To this end, two different types of sensors like accelerometers and laser triangulation sensor have been employed. It needs to be noted that besides the data characteristics of the aforementioned sensors, they record different quantities e.g. displacements, acceleration. However, the results are coherent regardless the sensors inherent differences (e.g. resolutions). Further, the measured quantities have different phase, resolutions, magnitudes, hence, the evaluation process requires appropriate data processing strategy. In a nutshell, the outcome of this study suggests that the responses (e.g. displacement, acceleration)

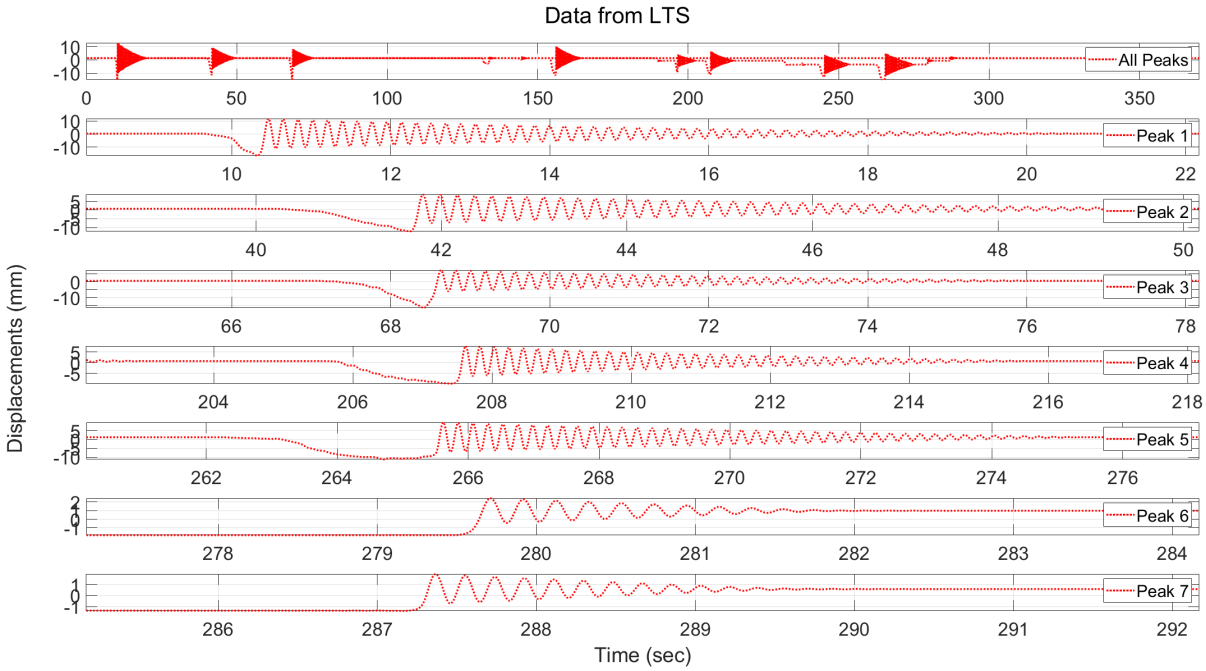


**Figure 7**: Time series data of displacements showing all peaks and selected time-windows under fixed-roller support condition

**Table 2**: Estimated damping ratios from acceleration and displacement data for fixed-roller support case

| Peaks | Damping ratio from acceleration | Damping ratio from displacement |
|---|---|---|
| Peak 1 | 0.016 | 0.017 |
| Peak 2 | 0.021 | 0.019 |
| Peak 3 | 0.021 | 0.022 |
| Peak 4 | 0.026 | 0.020 |
| Peak 5 | 0.020 | 0.017 |
| Peak 6 | 0.020 | 0.073 |
| Peak 7 | 0.047 | 0.055 |

of the structure may vary significantly depending on the type of input excitations and their magnitudes. Similar results are observed for both acceleration and displacements data. The variation of the maximum and minimum peak values are evaluated in time-domain and substantial changes in amplitudes are reported. Additionally, in frequency domain results, the changes of the resonant frequency has been noticed. Furthermore, the frequency shift for different time-windows are significant. In the last step, the damping ratio for both type of measured data have been evaluated and interestingly quite good match has been seen. In summary, it can be stated that the outcome of this study suggests that the variation of data and results provides more

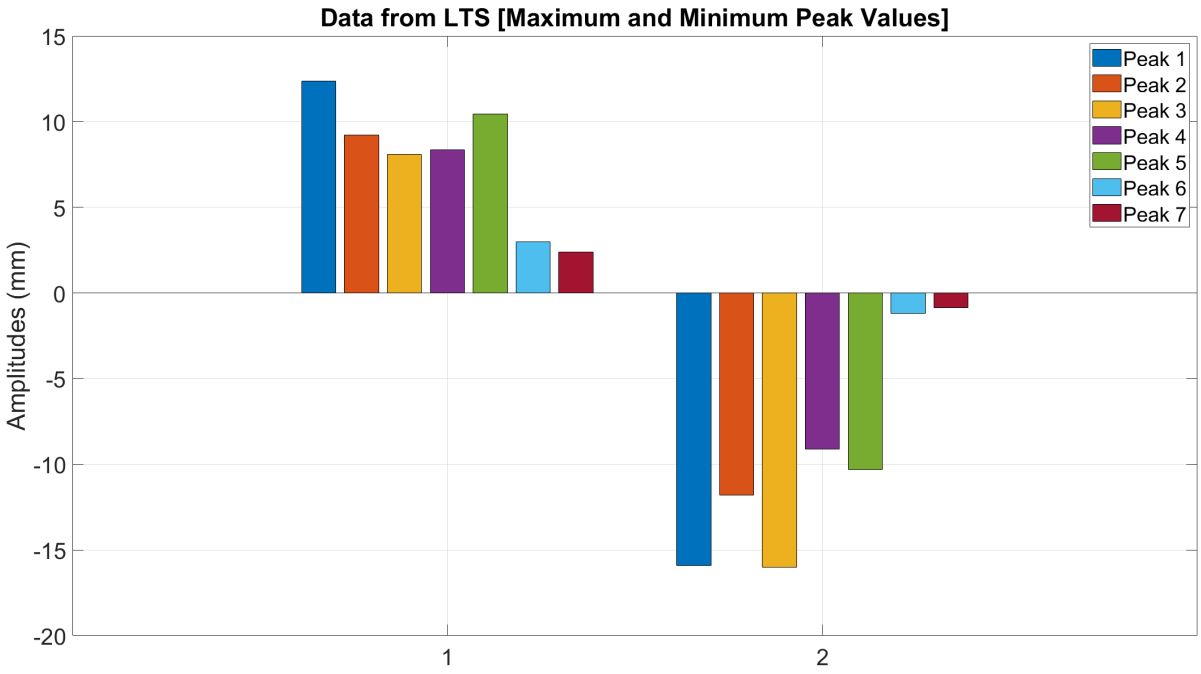


**Figure 8**: Maximum and minimum values of displacements under fixed-roller support condition

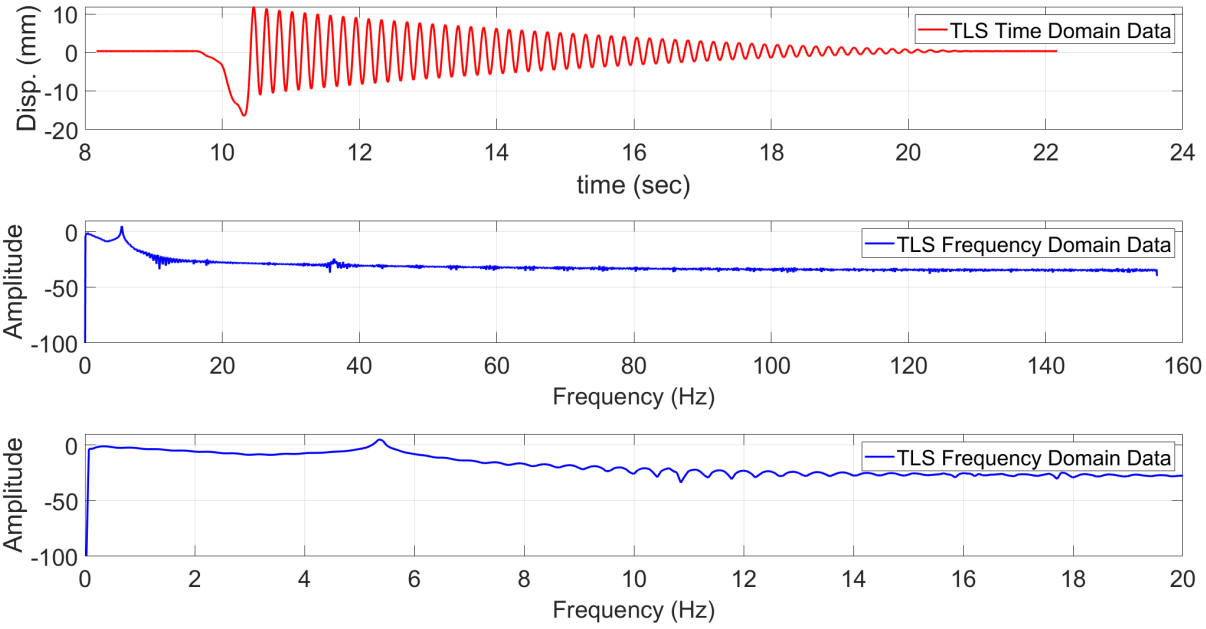


**Figure 9**: A sample set of results of reference (no extra weight on the bridge) case under fixed-roller support condition

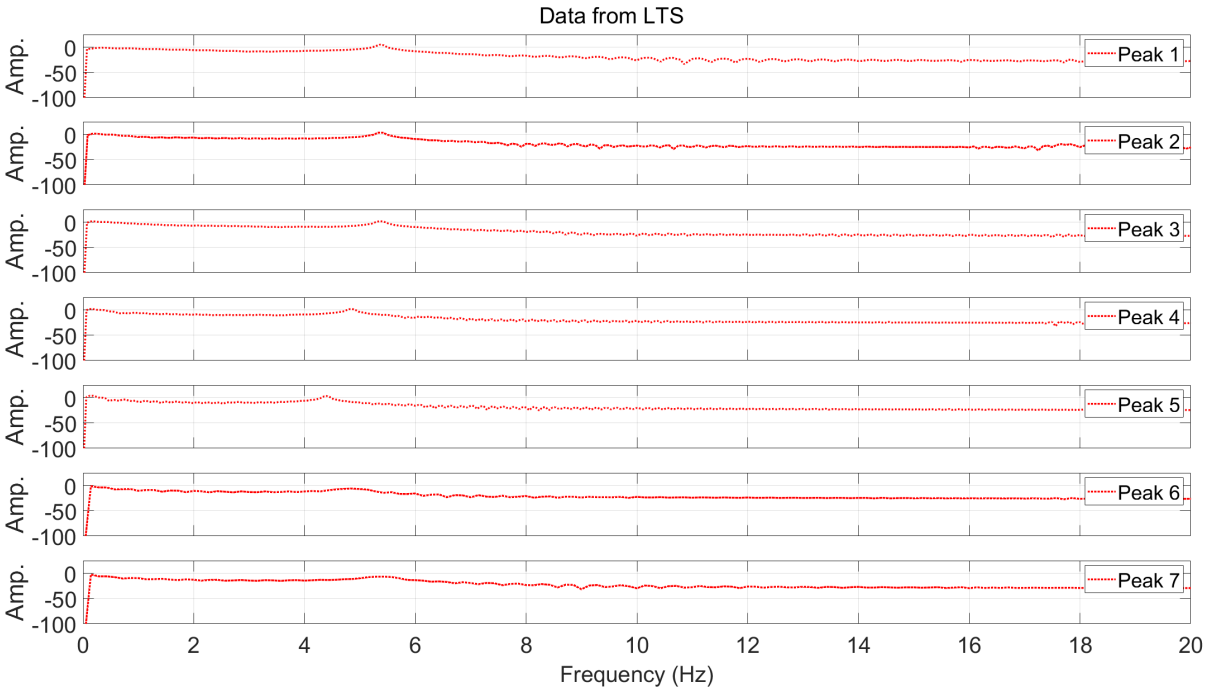


**Figure 10**: The comparison of spectrums of all considered time-windows under fixed-roller support condition

reliable information that is crucial to deal with numerous uncertainties, and obviously, to make overall decision in SHM.

## REFERENCES

[1] Dziedziech, K., Staszewski, W. J., and Uhl, T. Wavelet-based frequency response function: Comparative study of input excitation. *Shock and Vibration*, Vol. **2014**, pp. 1-11, 2014.

[2] Putra, A., and Mace, B. R. The effect of uncertainty in the excitation on the vibration input power to a structure. *Advances in Acoustics and Vibration*, Vol. **2013**, pp. 1-18, 2013.

[3] Lorenzoni, F., Casarin, F., Caldon, M., Islami, K., and Modena, C. (2016). Uncertainty quantification in structural health monitoring: Applications on cultural heritage buildings. Mechanical Systems and Signal Processing, 66–67, 268–281.

[4] Lam, H.-F. (1998). Structural Model Updating and Health Monitoring in the Presence of Modeling Uncertainties. PhD Thesis, Hong Kong University of Science and Technology, Hong Kong, 1-556.

[5] Miah, M. S., Chatzi, E. N., and Weber, F. Semi-active control for vibration mitigation of structural systems incorporating uncertainties. *Smart Materials and Structures*, **24**(5), 055016, 2015.

[6] Teimouri, H., Milani, A. S., Loeppky, J., and Seethaler, R. (2017). A Gaussian process–based approach to cope with uncertainty in structural health monitoring. Structural Health Monitoring, 16(2), 174–184.

[7] Sajedi, S. O., and Liang, X. (2021). Uncertainty-assisted deep vision structural health monitoring. Computer-Aided Civil and Infrastructure Engineering, 36(2), 126–142.

[8] Li, B. (2016). Uncertainty Quantification in Vibration-based Structural Health Monitoring using Bayesian Statistics. In University of California, Berkeley (Vol. 23, Issue 45). University of California, Berkeley.

[9] Sevieri, G., and De Falco, A. (2020). Dynamic structural health monitoring for concrete gravity dams based on the Bayesian inference. Journal of Civil Structural Health Monitoring, 10(2), 235–250.

[10] Hirai, K., and Mita, A. (2016). Uncertainty analysis of practical structural health monitoring systems currently employed for tall buildings consisting of small number of sensors. In T. Kundu (Ed.), Health Monitoring of Structural and Biological Systems 2016 (Vol. 9805, pp. 95–107). SPIE.

[11] Miah, M. S. and Kaliske, M. Monitoring and control of structures considering diverse uncertainties. Proc. SPIE 10970, *Sensors and Smart Structures Technologies for Civil, Mechanical, and Aerospace Systems*, **10970**,109701S, 2019.

[12] Mukhopadhyay, S. (2015). Structural Identification , Health Monitoring and Uncertainty Quantification under Incomplete Information with Minimal Requirements for Identifiability. COLUMBIA UNIVERSITY.

[13] Liu, G., Mao, Z., and Luo, J. (2015). Damage detection with interval analysis for uncertainties quantification. Proceedings of the Second International Conference on Performance-Based and Life-Cycle Structural Engineering (PLSE 2015), 30(1), 272–281.

[14] Asgrimsson, D. S. (2019). Quantifying uncertainty in structural condition with Bayesian deep learning A study on the Z-24 bridge benchmark. 50.

[15] Bull, L. A., Gardner, P., Rogers, T. J., Cross, E. J., Dervilis, N., and Worden, K. (2021). Probabilistic Inference for Structural Health Monitoring: New Modes of Learning from Data. ASCE-ASME Journal of Risk and Uncertainty in Engineering Systems, Part A: Civil Engineering, 7(1), 03120003.

[16] Drira, S., Pai, S. G. S., and Smith, I. F. C. (2021). Uncertainties in Structural Behavior for Model-Based Occupant Localization Using Floor Vibrations. Frontiers in Built Environment, 7(April), 1–21.

[17] Liu, A., Wang, L., Bornn, L., and Farrar, C. (2019). Robust structural health monitoring under environmental and operational uncertainty with switching state-space autoregressive models. Structural Health Monitoring, 18(2), 435–453.

[18] Caspani, V. F., Tonelli, D., Poli, F., and Zonta, D. (2022). Designing a Structural Health Monitoring System Accounting for Temperature Compensation. Infrastructures, 7(1).

[19] Sankararaman, S., and Goebel, K. (2015). Uncertainty in prognostics and systems health management. International Journal of Prognostics and Health Management, 6, 1–14.

[20] GOKCE, H. B. (2012). Structural Identification Through Monitoring, Modeling And Predictive Analysis Under Uncertainty (Issue 2012) [University of Central Florida].

[21] Jenkel, C., Graf, W., and Sickert, J.-U. Structural health monitoring under consideration of uncertain data. *LS-DYNA Anwenderforum*, 1–10, 2008.

[22] Papagiannopoulos, G. A., Hatzigeorgiou, G. D. (2011). On the use of the half-power bandwidth method to estimate damping in building structures. Soil Dynamics and Earthquake Engineering, 31(7), 1075–1079.